This is the accepted manuscript (postprint) of the following article:
E. Salahinejad, M.J. Hadianfard, D.D. Macdonald, S. Sharifia(asl), M. Mozafari, K.J. Walker, A. Tahmasbi Rad, S.V. Madihally, D. Vashaee, L. Tayebi, *Surface Modification of Stainless Steel Orthopedic Implants by Sol–Gel $ZrTiO_4$ and $ZrTiO_4$–PMMA Coatings*, Journal of Biomedical Nanotechnology, 9 (2013) 1327-1335.
http://dx.doi.org/10.1166/jbn.2013.1619

Surface modification of stainless steel orthopedic implants by sol–gel $ZrTiO_4$ and $ZrTiO_4$–PMMA coatings

E. Salahinejad [a,b,c], M.J. Hadianfard [c], D.D. Macdonald [b,d], S. Sharifi(Asl) [b], M. Mozafari [a,b], K.J. Walker [e], A. Tahmasbi Rad [a], S.V. Madihally [e], D. Vashaee [f], L. Tayebi [a,e,**]

[a] Helmerich Advanced Technology Research Center, School of Materials Science and Engineering, Oklahoma State University, OK 74106, USA

[b] Center for Electrochemical Science and Technology, Department of Materials Science and Engineering, Pennsylvania State University, University Park, PA 16802, USA

[c] Department of Materials Science and Engineering, School of Engineering, Shiraz University, Zand Blvd., 7134851154, Shiraz, Iran

[d] Center for Research Excellence in Corrosion, King Fahd University of Petroleum and Minerals, Dhahran 31261, Saudi Arabia

[e] School of Chemical Engineering, Oklahoma State University, Stillwater, OK 74078, USA

[f] Helmerich Advanced Technology Research Center, School of Electrical and Computer Engineering, Oklahoma State University, OK 74106, USA

Abstract

In this paper, the biocompatibility of a medical-grade stainless steel coated with sol–gel derived, nanostructured inorganic $ZrTiO_4$ and hybrid $ZrTiO_4$–PMMA thin films is correlated with surface characteristics. The surfaces of the samples are characterized by atomic force microscopy, the sessile drop technique, and electrochemical corrosion experiments. The viability of adult human mesenchymal stem cells on the surfaces after one day of culture is also assessed quantitatively and morphologically. According to the results, both of the coatings improve the hydrophilicity, corrosion resistance, and thereby cytocompatibility of the substrate. Despite the higher corrosion protection by the hybrid coating, the sample coated with the inorganic thin film exhibits a better cell response, suggesting the domination

* Corresponding author: *E-mail address*: lobat.tayebi@okstate.edu (L. Tayebi)

This is the accepted manuscript (postprint) of the following article:
E. Salahinejad, M.J. Hadianfard, D.D. Macdonald, S. Sharifia(asl), M. Mozafari, K.J. Walker, A. Tahmasbi Rad, S.V. Madihally, D. Vashaee, L. Tayebi, *Surface Modification of Stainless Steel Orthopedic Implants by Sol–Gel $ZrTiO_4$ and $ZrTiO_4$–PMMA Coatings*, Journal of Biomedical Nanotechnology, 9 (2013) 1327-1335.
http://dx.doi.org/10.1166/jbn.2013.1619

of wettability. In summary, the $ZrTiO_4$-based sol–gel films can be considered to improve the biocompatibility of metallic implants.

Keywords: Sol–gel coating; Water contact angle; Corrosion resistance; Cytocompatibility; Zirconium titanate

1. Introduction

Although various alloys fulfill the mechanical properties required for orthopedic implants, only a few satisfy the biological requirements of corrosion resistance and, more critically, biocompatibility, simultaneously. Unfortunately, so far no metallic biomaterial has been found to offer all of the technical and biological functions in the body. One effective approach to adjust conventional biomaterials to the clinical needs is surface modification. Coating, as one of these methods, not only can increase the corrosion resistance of the implant, but also can improve the implant-tissue interaction, affecting biological responses like bioactivity and cytocompatibility [1].

Stainless steels, typically AISI 316L, are traditionally used in fabricating orthopedic implants, especially as bone fixation (bone plates, screw wire min-plate, etc.), spinal fixation, catheters, and cardiovascular (terminal, stent) applications [2]. However, the corrosion reaction of this alloy in the body fluid can lead to the early failure of the implant and can interfere with the functioning of adjacent tissues. Among various methods used to prepare coatings, the sol–gel deposition process has advantages, such as high homogeneity, low sintering temperature, and simplicity in the coating of complex shapes [3]. Although widespread studies have been conducted on titania and zirconia coating of stainless steels, little systematic work has been reported on sol–gel zirconium titanate ($ZrTiO_4$) coatings in

This is the accepted manuscript (postprint) of the following article:
E. Salahinejad, M.J. Hadianfard, D.D. Macdonald, S. Sharifia(asl), M. Mozafari, K.J. Walker, A. Tahmasbi Rad, S.V. Madihally, D. Vashaee, L. Tayebi, *Surface Modification of Stainless Steel Orthopedic Implants by Sol–Gel $ZrTiO_4$ and $ZrTiO_4$–PMMA Coatings*, Journal of Biomedical Nanotechnology, 9 (2013) 1327-1335.
http://dx.doi.org/10.1166/jbn.2013.1619

the biomedical field. Typically, Devi et al. [4] investigated the structure and bioactivity of a stainless steel coated with $ZrTiO_4$ by a non-hydrolytic sol–gel method. Additionally, the physical, mechanical, and tribological behaviors of magnetron-sputtered $ZrTiO_4$ coatings for orthopedic and dental implants were reported [5].

To the best of our knowledge, the biocompatibility of $ZrTiO_4$-based coatings, including inorganic and organic-inorganic hybrid coatings, has not been studied to date. In this paper, the cell viability of inorganic $ZrTiO_4$ and hybrid $ZrTiO_4$–PMMA thin films prepared by an aqueous particulate sol–gel method on stainless steel is evaluated. Furthermore, the cytocompatibility behavior is correlated with the roughness, wettability, and corrosion resistance of the samples.

2. Experimental procedures

2.1. Sample preparation

Medical-grade, austenitic stainless steel substrates were surface-prepared by grinding via No. 180-3000 emery papers, polishing with 1 and 0.1 μm alumina powders, and ultrasonically cleaning in acetone, ethanol, and distilled water. Two types of mono-layer, sol–gel derived coatings were deposited on the substrates: $ZrTiO_4$ and $ZrTiO_4$–PMMA. To do so, an equal molar solution of $ZrCl_4$ (Alfa Aesar, 99.5 %) and $TiCl_4$ (Alfa Aesar, 99.99 %) was prepared in deionized water. Then, by dropwise addition of NaOH solution, the pH of the solution was increased to 7 with the formation of a hydrogel. To remove chloride ion, the hydrogel was repeatedly rinsed with deionized water and centrifuged at 6000 rpm. Afterward, 75 mL of deionized water and 2 wt.% carboxymethyl cellulose (CMC, sodium salt, Alfa Aesar) as a dispersing agent [6–8] were added to the centrifuged product. To prepare the

This is the accepted manuscript (postprint) of the following article:
E. Salahinejad, M.J. Hadianfard, D.D. Macdonald, S. Sharifia(asl), M. Mozafari, K.J. Walker, A. Tahmasbi Rad, S.V. Madihally, D. Vashaee, L. Tayebi, *Surface Modification of Stainless Steel Orthopedic Implants by Sol–Gel $ZrTiO_4$ and $ZrTiO_4$–PMMA Coatings*, Journal of Biomedical Nanotechnology, 9 (2013) 1327-1335.
http://dx.doi.org/10.1166/jbn.2013.1619

hybrid $ZrTiO_4$–10 vol.% PMMA coating, the proper amount of polymethyl methacrylate (PMMA, Alfa Aesar, average molecular weight: 550 gr/mol) was dissolved in acetone and added to the nanoparticles-containing sol prepared by the above procedure. The sols were separately spin coated on the substrate at a speed of 3000 rpm for 60 sec. The inorganic and hybrid coatings were sintered at 700 °C and 150 °C for 1 h, respectively, leading to the preparation of homogeneous thin films of almost 50 nm in thickness, as measured by a NanoSpec 3000 system (Nanometrics) using a small spot spectroscopic reflectometer.

2.2. Sample characterization

2.2.1. Atomic force microscopy

The sample surfaces were studied morphologically using a Veeco Multimode atomic force microscope (AFM, Bruker AXS) to evaluate roughness. AFM allows determination of the surface roughness by considering the distribution curve of relative height among points in the scanning area and calculating the average value with respect to a central plane. By using the DI NanoScope 7.20 software, the average roughness value of the substrate and films was determined over areas of 5×5 μm^2.

2.2.2. Static contact angle measurements

To compare the wettability and hydrophilicity of the specimens, the sessile drop technique was employed under static conditions by settling a deionized water droplet of 10 µL onto the surfaces, allowing it to spread until equilibrium is reached, and analyzing the profile to extract the angle formed at the three-phase interface. In this procedure, it is

This is the accepted manuscript (postprint) of the following article:
E. Salahinejad, M.J. Hadianfard, D.D. Macdonald, S. Sharifia(asl), M. Mozafari, K.J. Walker, A. Tahmasbi Rad, S.V. Madihally, D. Vashaee, L. Tayebi, *Surface Modification of Stainless Steel Orthopedic Implants by Sol–Gel $ZrTiO_4$ and $ZrTiO_4$–PMMA Coatings*, Journal of Biomedical Nanotechnology, 9 (2013) 1327-1335.
http://dx.doi.org/10.1166/jbn.2013.1619

presumed that the droplet is axisymmetric and that its shape is dominated by interfacial tensions [9,10].

2.2.3. Electrochemical corrosion evaluations

The *in vitro* electrochemical corrosion behavior of the samples was investigated in the simulated body fluid (SBF) proposed by Kokubo and Takadama [11] at a pH value of 7.4 under the naturally aerated condition, using a Gamry PC3/300 Potentiostat/Galvanostat/ZRA. Table 1 compares the ion concentration of SBF and human blood plasma. A platinum wire and saturated calomel electrode (SCE) were employed as the auxiliary and reference electrodes, respectively. The samples were firstly immersed in SBF for 1 h to obtain a steady-state open circuit potential (*ocp*). Subsequently, anodic potentiodynamic polarization curves were obtained at a scan rate of 1 mVs^{-1} from -0.1 V vs. *ocp* to the transpassive potential in the same solution. Electrochemical impedance spectroscopic measurements were also performed over ten frequency decades from 5 kHz to 10 mHz with an excitation potential amplitude of 10 mV at the *ocp*. All of the electrochemical results were analyzed by using the Gamry Echem Analyst (Version 5.50) software.

2.3. Cytocompatibility assessments

Adult human mesenchymal stem cells (hMSC, Lonza Walkersville Inc., MD, USA) were cultured in a mesenchymal stem cell basal medium (MSCGM, Lonza) with other supplements, as recommended by the protocol from Lonza Walkersville. The cells were incubated at 37°C in a 5% CO_2/95% air atmosphere with the medium being exchanged every 3 to 4 days. The cells proliferated normally in the manner of size, shape, and confluency.

This is the accepted manuscript (postprint) of the following article:
E. Salahinejad, M.J. Hadianfard, D.D. Macdonald, S. Sharifia(asl), M. Mozafari, K.J. Walker, A. Tahmasbi Rad, S.V. Madihally, D. Vashaee, L. Tayebi, *Surface Modification of Stainless Steel Orthopedic Implants by Sol–Gel $ZrTiO_4$ and $ZrTiO_4$–PMMA Coatings*, Journal of Biomedical Nanotechnology, 9 (2013) 1327-1335.
http://dx.doi.org/10.1166/jbn.2013.1619

Upon confluence, the cells were removed from the plate with Clonetics Trypsin-EDTA (Lonza Walkersville). The cells then underwent centrifugation at 300 g for five minutes and were suspended in the growth medium. Viable cell counting was done using Trypan blue dye exclusion assay. Next, the cells were stained using anamine-reactive, colorless, non-fluorescent dye that diffuses into the cytoplasm of the cells, 5-(and-6)-carboxyfluoresceindiacetate, succinimidyl ester (CFDA-SE) -mixed isomers obtained from Invitrogen Corp. Carlsbad, CA, USA.

All of the samples were sterilized by autoclaving at 134°C for 20 min and placed in a 24-well plate pre-coated with bovine serum albumin. Quadruplicate samples were used for each condition. Then, ten thousand cells were seeded onto the tissue culture plastic (TCP) surface and each substrate. A similar number of the cells in suspension were also frozen for the analysis of the initial CFDA-SE content. To achieve a uniform distribution of the cells on the samples, a concentrated (500,000 cells/mL) cell suspension was placed at different locations on each sample and allowed to attach for 30 min prior to adding the growth medium. After one day, the cell-containing samples were fixed in 3.7% formaldehyde for 30 minutes at room temperature. The samples were dried using ethanol, followed by brief vacuum drying, and were then sputter coated with gold at 40 mA prior to examination in a scanning electron microscope (SEM, Hitachi S-4800).

Cell viability after one day was assessed by two approaches: first, 100 µL of spent media collected on that day were used to analyze cell viability indirectly. Next, the specimens containing the cells were washed in MSCGM, and cytoplasmic CFDA-SE stained was extracted from the live cells by three cycles of repeated freezing and thawing. The CFDA-SE content in the spent medium and the cytoplasm was assessed by fluorescence intensity in a

This is the accepted manuscript (postprint) of the following article:
E. Salahinejad, M.J. Hadianfard, D.D. Macdonald, S. Sharifia(asl), M. Mozafari, K.J. Walker, A. Tahmasbi Rad, S.V. Madihally, D. Vashaee, L. Tayebi, *Surface Modification of Stainless Steel Orthopedic Implants by Sol–Gel $ZrTiO_4$ and $ZrTiO_4$–PMMA Coatings*, Journal of Biomedical Nanotechnology, 9 (2013) 1327-1335.
http://dx.doi.org/10.1166/jbn.2013.1619

Gemini XS spectrofluorometer (MDS technologies, Santa Clara, CA) at the excitation and emission wavelengths of 485 nm and 525 nm, respectively. All fluorescence values for the samples were normalized to the TCP for comparison.

3. Results and discussion

3.1. AFM studies

The two- and three-dimensional AFM images of the sample surfaces are presented in Fig. 1. Aligned scratches caused by mechanical polishing can be seen on the surface of the polished, uncoated stainless steel (Fig. 1a). The sol–gel derived coatings are smooth, uniform, and dense, as can be observed in Figs. 1b and 1c. On the surface of the $ZrTiO_4$ and $ZrTiO_4$–PMMA coatings, there are globular nanoparticles with an average diameter of 50 and 10 nm, respectively. The roughness value of the samples is 14±2, 11±2, and 7±3 nm for the substrate uncoated and coated with the organic and hybrid coatings, respectively. The slightly higher roughness value of the inorganic film compared with the organic-inorganic hybrid film is due to the higher sintering temperature used in preparing the former. In the course of sintering, nanoparticles grow [6,8] and start appearing on the surface, due to mass transfer caused by transformation from a glass state to a crystalline one [12]. Indeed, initially a strained continuous layer is formed on the substrate and then the strain is released by the formation of three-dimensional islands on that layer (Stranski–Krastanov growth model) [13,14], thereby providing rough films with a large number of valleys and mountains. According to Ref. [6], the crystallization temperature of the amorphous nanoparticles synthesized by the sol–gel process is about 700 °C. Thus, considering the used firing temperatures, the nanoparticles in

This is the accepted manuscript (postprint) of the following article:
E. Salahinejad, M.J. Hadianfard, D.D. Macdonald, S. Sharifia(asl), M. Mozafari, K.J. Walker, A. Tahmasbi Rad, S.V. Madihally, D. Vashaee, L. Tayebi, *Surface Modification of Stainless Steel Orthopedic Implants by Sol–Gel $ZrTiO_4$ and $ZrTiO_4$–PMMA Coatings*, Journal of Biomedical Nanotechnology, 9 (2013) 1327-1335.
http://dx.doi.org/10.1166/jbn.2013.1619

the $ZrTiO_4$ and $ZrTiO_4$–PMMA thin films are crystalline and amorphous in structure, respectively.

3.2. Wettability

Wettability, which is defined as the tendency for a liquid to spread on a solid substrate, is one of the basic features of surfaces and plays a prime role in biological responses, typically in the interaction of the implant with natural bone tissues [15,16]. Fig. 3 shows an optical photo of a water droplet on the uncoated and coated steel substrates. The measured contact angles formed at the three-phase interface are 82, 28, and 50 º for the stainless steel uncoated and coated with the $ZrTiO_4$ and $ZrTiO_4$–PMMA coatings, respectively. A lower contact angle or better spread is indicative of a higher hydrophilicity. Thus, it is concluded that the coatings applied induce hydrophilicity to the stainless steel substrate.

The hydrophilic nature of zirconium titanate is attributed to the presence of highly negatively charged hydroxyl groups on the surface [4]. Some water molecules are physically and chemically adsorbed on the surface and react with the metal oxide ceramic, forming Ti–OH and Zr–OH. Interactions between H_2O and OH^-, via van der Waals forces and hydrogen bonds, lead to a better spread of water on the surface. It is believed that in this mechanism, the coordination of water molecule into the oxygen vacancy sites in the surface of the ceramic substrate plays a critical role in determining the hydroxyl content and thereby the hydrophilicity [17].

The higher contact angle formed on the hybrid $ZrTiO_4$–PMMA film than on the $ZrTiO_4$ film is due to the hydrophobic nature of PMMA in comparison with $ZrTiO_4$. The structure of this polymer contains hydrophobic functional groups like α-methyl, ester methyl,

This is the accepted manuscript (postprint) of the following article:
E. Salahinejad, M.J. Hadianfard, D.D. Macdonald, S. Sharifia(asl), M. Mozafari, K.J. Walker, A. Tahmasbi Rad, S.V. Madihally, D. Vashaee, L. Tayebi, *Surface Modification of Stainless Steel Orthopedic Implants by Sol–Gel $ZrTiO_4$ and $ZrTiO_4$–PMMA Coatings*, Journal of Biomedical Nanotechnology, 9 (2013) 1327-1335.
http://dx.doi.org/10.1166/jbn.2013.1619

and methylene and also hydrophilic functional groups like carbonyl. Although the surface of PMMA in contact with water can comprise hydrophilic and hydrophobic domains at a sub-nanometric scale, PMMA essentially presets a hydrophilic behavior, albeit with an intrinsic contact angle below 90º [18].

3.3. Corrosion evaluations

Fig. 3 represents the potentiodynamic polarization curve of the uncoated and coated samples. The differences in the polarization curves, a result of sol–gel coating, are detailed as below. Firstly, the corrosion potential of the coated samples is higher than that of the substrate and also the hybrid coating provides a nobler potential than the inorganic coating. Secondly, the corrosion current density decreases in this order: substrate > $ZrTiO_4$ > $ZrTiO_4$–PMMA. From the shift in the corrosion current density, the protection efficiency (P) of the sol–gel coatings is calculated by [19]:

$$P = 100\ (1 - i_{cor}/i^0_{cor}) \quad (1)$$

where i_{cor} and i^0_{cor} denote the corrosion current density of the coated and uncoated samples, respectively. The protection efficiency of the inorganic and hybrid coatings was determined to be 84 and 95 %, respectively. Thirdly, in contrast to the substrate, the coated samples exhibit obvious "passivation-like" regions, where the $ZrTiO_4$–PMMA thin film, compared with the $ZrTiO_4$ coating, yields a lower passivation current density (better passivity). Finally, from the breakdown potential and passive potential range, it can be concluded that the stability of the passive region for the hybrid-coated specimen is more than for the inorganic-coated sample. Hence, according to the polarization tests, the anti-corrosion behavior is

This is the accepted manuscript (postprint) of the following article:
E. Salahinejad, M.J. Hadianfard, D.D. Macdonald, S. Sharifia(asl), M. Mozafari, K.J. Walker, A. Tahmasbi Rad, S.V. Madihally, D. Vashaee, L. Tayebi, *Surface Modification of Stainless Steel Orthopedic Implants by Sol–Gel $ZrTiO_4$ and $ZrTiO_4$–PMMA Coatings*, Journal of Biomedical Nanotechnology, 9 (2013) 1327-1335.
http://dx.doi.org/10.1166/jbn.2013.1619

improved in this order: substrate < $ZrTiO_4$ < $ZrTiO_4$–PMMA, where the coatings act as a physical protective barrier for blocking the electrochemical processes.

The Nyquist and Bode impedance plots of the samples are shown in Fig. 4. It can be seen that all of the samples present a similar impedance behavior under the chosen test conditions. The Nyquist diagrams, signifying considerable values of the real and imaginary impedance at low frequencies, and also the time constant observed in the Bode phase angle plots are typical of passive systems. Typically, an increase in the phase angle up to 85° for the hybrid-coated specimen and up to 80° for the two other samples is observed, inferring a highly capacitive behavior up to almost 40 Hz. Also, some conductivity is clear at higher frequencies, as can be seen from the decrease in the phase angle. According to the Bode impedance plots, the value of impedance modulus increases in this order: substrate < $ZrTiO_4$ < $ZrTiO_4$–PMMA. Considering the fact that value of impedance is inversely proportional to the corrosion rate, the hybrid-coated sample exhibits the lowest corrosion rate and the uncoated sample presents the highest susceptibility towards corrosion. This confirms the corrosion protection of the substrate by the coatings, as realized from the polarization tests.

Immersion of a metallic electrode into a corrosive electrolyte develops an oxide film on the exposed surface. The theory of the ennoblement of passive metals upon prolonged exposure under open circuit conditions is now well-developed and it shows that the positive drift in the potential occurs, because of a progressive thickening of the barrier oxide layer [20]. Considering the impedance spectral features and surface film, an equivalent electrical circuit (Fig. 4d) was used for the quantitative analyses of the impedance spectra. Fitting of the model to the data was accomplished by using a nonlinear least-squares method, resulting in the low values of residual error (Table 2). Due to the distribution of relaxation times

This is the accepted manuscript (postprint) of the following article:
E. Salahinejad, M.J. Hadianfard, D.D. Macdonald, S. Sharifia(asl), M. Mozafari, K.J. Walker, A. Tahmasbi Rad, S.V. Madihally, D. Vashaee, L. Tayebi, *Surface Modification of Stainless Steel Orthopedic Implants by Sol–Gel $ZrTiO_4$ and $ZrTiO_4$–PMMA Coatings*, Journal of Biomedical Nanotechnology, 9 (2013) 1327-1335.
http://dx.doi.org/10.1166/jbn.2013.1619

resulting from inhomogeneities on the electrode surface at nano/micro scale (like roughness, porosity, adsorption, and/or diffusion) [21,22], the use of constant phase elements (CPEs), rather than pure capacitors, improved the fitting. The impedance (Z_{CPE}) of a CPE is expressed as:

$$Z_{CPE} = \frac{1}{Q(j\omega)^n} \quad (2)$$

where Q is the capacitance in F, ω is the angular frequency ($\omega = 2\pi f$; f is the frequency in Hz), j is $(-1)^{0.5}$, and n is an empirical exponent that is less than one describing the deviation of the real system from that of an ideal capacitor. Therefore, the total impedance for the proposed circuit is:

$$Z = R_{sol} + (Q_c(j\omega)^{n_c} + \frac{1 + R_{ct}Q_{dl}(j\omega)^{n_{dl}}}{R_{po} + R_{ct} + R_{po}R_{ct}Q_{dl}(j\omega)^{n_{dl}}}) \quad (3)$$

where R_{sol} is the electrolyte resistance, R_{po} is the resistance of film pores, R_{ct} is the charge transfer resistance. CPE_c (Q_c, n_c) and CPE_{dl} (Q_{dl}, n_{dl}) correspond to the geometric capacitance of the film and double layer, respectively.

The equivalent electrical circuit parameters are listed in Table 2. The polarization resistance (R_p), which is the sum of all the ohmic resistances, is a measure of the resistance of the surface to general corrosion as expressed via the Stern-Geary equation and can be regarded as a criterion for judging the corrosion rate and ion release rate: the higher R_p, the lower corrosion rate under the test conditions. Thus, the corrosion rate and ion release rate show an increasing trend in this order: $ZrTiO_4$–PMMA < $ZrTiO_4$ < substrate, which is in good agreement with the potentiodynamic polarization results. Concerning the CPCs, as the value of the exponent n is close to one, they can be regarded as capacitors. A lower Q_1 value

This is the accepted manuscript (postprint) of the following article:
E. Salahinejad, M.J. Hadianfard, D.D. Macdonald, S. Sharifia(asl), M. Mozafari, K.J. Walker, A. Tahmasbi Rad, S.V. Madihally, D. Vashaee, L. Tayebi, *Surface Modification of Stainless Steel Orthopedic Implants by Sol–Gel $ZrTiO_4$ and $ZrTiO_4$–PMMA Coatings*, Journal of Biomedical Nanotechnology, 9 (2013) 1327-1335.
http://dx.doi.org/10.1166/jbn.2013.1619

suggests a more stable surface layer at high frequency. The capacitance (C) is calculated by the following equation:

$$C = \varepsilon \varepsilon_0 A/l \quad (4)$$

where ε is the dielectric constant, ε_0 is the permittivity of free space, A is the surface area, and l is the thickness of the film. It can be seen that the capacitance of the inorganic film is higher than that of the hybrid film. As well as the different capacitance of the materials (the role of the addition of PMMA), the porous structure of the inorganic coating with a higher hydrophilicity, as shown by the sessile drop technique, tends to absorb more water than the hybrid film. Accordingly, the water uptake increases the dielectric constant of the coating, because the dielectric constant of water is higher than organic and inorganic materials [23]. Also, the higher porosity of the inorganic film, as discussed below, provides a more surface area and thereby increases the capacitance, based on Eq. (4).

As noted above, sol–gel coatings as geometric blocking layers impede the access of the electrolyte to the metal surface and hence improve the corrosion resistance. This higher protection efficiency of the hybrid coating compared with the inorganic coating can be attributed to its lower defect density and hydrophilicity. In contrast to organic coatings, which are permeable to water and oxygen, sol–gel coatings only can corrode through their defects allowing the electrolyte access to the metal surface [24]. The porosity level (P) signifying the area exposed to the electrolyte can be estimated by the following equation [25]:

$$P = \frac{R_{ps}}{R_p} \times 10^{-\left|\frac{\Delta E_{corr}}{b_a}\right|} \times 100 \quad (5)$$

where R_{ps} and R_p are the polarization resistance of the substrate and coating, respectively, b_a is the Tafel slope of the substrate, and ΔE_{corr} is the difference in the corrosion potential of the

This is the accepted manuscript (postprint) of the following article:
E. Salahinejad, M.J. Hadianfard, D.D. Macdonald, S. Sharifia(asl), M. Mozafari, K.J. Walker, A. Tahmasbi Rad, S.V. Madihally, D. Vashaee, L. Tayebi, *Surface Modification of Stainless Steel Orthopedic Implants by Sol–Gel $ZrTiO_4$ and $ZrTiO_4$–PMMA Coatings*, Journal of Biomedical Nanotechnology, 9 (2013) 1327-1335.
http://dx.doi.org/10.1166/jbn.2013.1619

coated and uncoated substrates. According to the results, the porosity content of the sample coated with the $ZrTiO_4$ and $ZrTiO_4$–PMMA thin films was calculated to be 22 and 8 %, respectively. Essentially, the nanoparticles processed by the sol–gel method develop a thin film containing nanosized porosities. During sintering of the coating, PMMA as the low-melting point organic component fills the void volume and hence decreases the porosity, thereby producing a denser barrier against the electrochemical reactions. On the other hand, as indicated above, due to the addition of PMMA, the hybrid thin film is more hydrophobic than the inorganic coating. This feature suppresses the electrolyte permeation into the coating structure through defects like probable cracks and interconnecting porosities and thereby impedes the electrolyte access to the metal/coating interface [26]. It is also noteworthy that the probability of cracking in hybrid coatings, due to their higher flexibility, is less than in oxide coatings [27].

3.4. Cell viability

By pre-staining the cells with CFDA-SE, the viability of hMSCs on the specimens was evaluated after one day of culture. According to the cytoplasmic contents obtained from the freeze/thaw cycle (Fig. 5), the cell viability for all of the samples is considerable and is comparable to TCP, suggesting that they are not toxic to the cells. The supernatants collected after one day of culture also confirmed cytocompatibility of the samples. It can be seen that the viability shows a slight decline in this order: $ZrTiO_4$ > $ZrTiO_4$–PMMA > substrate.

To evaluate the cell's spreading and morphology on the samples, SEM micrographs of the cell-cultured surfaces are depicted in Figs. 6 and 7. As can be observed in the SEM micrographs, the cells are well-spread onto the surfaces with numerous lamellipodia and

This is the accepted manuscript (postprint) of the following article:
E. Salahinejad, M.J. Hadianfard, D.D. Macdonald, S. Sharifia(asl), M. Mozafari, K.J. Walker, A. Tahmasbi Rad, S.V. Madihally, D. Vashaee, L. Tayebi, *Surface Modification of Stainless Steel Orthopedic Implants by Sol–Gel $ZrTiO_4$ and $ZrTiO_4$–PMMA Coatings*, Journal of Biomedical Nanotechnology, 9 (2013) 1327-1335.
http://dx.doi.org/10.1166/jbn.2013.1619

filopodia. This desirable feature is indicative of a good cellular migration and attachment, implying the biocompatibility of the implants, as realized by the quantitative analysis. Nonetheless, the number and distribution uniformity of the cells are enhanced (Fig. 6) and the cell's spreading capacity and morphology are improved (Fig. 7) in this order: substrate < $ZrTiO_4$–PMMA < $ZrTiO_4$. Accordingly, based on both of the quantitative and microscopic studies, biocompatibility is improved in this order: substrate < $ZrTiO_4$–PMMA < $ZrTiO_4$.

Biocompatibility of a material, which can be characterized by cellular responses in contact with the implant, is fundamentally affected by its hydrophilicity, roughness, and ion release rate [28]. Once a biomaterial is implanted in the body, the interaction of water molecules with the implant surface occurs within nanoseconds [15,28]. The surface properties of the implant, especially its surface free energy or hydrophilicity, determine the character of the interaction and bonding between the substrate and water molecules. This affects the organization of water molecules and the cellular response. Typically, water molecules that attach to the surface by hydrogen bonding encourage the interaction of specific molecules like proteins which are involved in the cell/substrate interaction [29]. Interactions between proteins and their specific receptors induce signal transduction, thereby affecting cell adhesion, growth, and differentiation [30]. In this circumstance, hydrophilic surfaces, especially moderately hydrophilic ones, provide for better protein adsorption, cell spreading, cell proliferation, and biocompatibility [16,31,32]. On the effect of roughness on biocompatibility and cell adhesion, there is much disagreement. In this regard, Hong et al. [33] showed that rough surfaces lead to a higher cell adhesion compared to smooth surfaces, since a more surface area induces a more reactivity of cells and substrate. Nonetheless, Ponsonnet et al. [34] reported that there is a roughness threshold, between 0.08 and 1 μm,

This is the accepted manuscript (postprint) of the following article:
E. Salahinejad, M.J. Hadianfard, D.D. Macdonald, S. Sharifia(asl), M. Mozafari, K.J. Walker, A. Tahmasbi Rad, S.V. Madihally, D. Vashaee, L. Tayebi, *Surface Modification of Stainless Steel Orthopedic Implants by Sol–Gel $ZrTiO_4$ and $ZrTiO_4$–PMMA Coatings*, Journal of Biomedical Nanotechnology, 9 (2013) 1327-1335.
http://dx.doi.org/10.1166/jbn.2013.1619

over which cell proliferation is retarded. Bigerelle et al. [35] found that when roughness is less than the cell scale (micron), isotropic smooth surfaces are preferred for the cell adhesion. On the contrary, in the case of roughness higher than the cell scale, cells take advantage of isotropic rough surfaces. Moreover, the biocompatibility of a material is affected by the amount and toxicity of the substrate's constituent elements and also by the ion release rate or corrosion resistance, since corrosion products can react toxically with the cells.

In this study, since the roughness values of the samples are very close, the roughness has no contribution to the difference observed in the biocompatibility of the specimens. Thus, the differences can be explained by the effect of the wettability and corrosion behavior. The better cell viability of the coated samples, compared with the uncoated stainless steel is attributed to the improvement in the hydrophilicity and corrosion resistance of the substrate, as shown in Figs. 2, 3, and 4. Although the corrosion rate and thereby ion release rate of the sample coated with the $ZrTiO_4$–PMMA film are less than those of the sample coated with the $ZrTiO_4$ film, the latter exhibits a better cell viability. Considering the more wettability of the inorganic-coated sample compared with the hybrid-coated sample (Fig. 2), it can be inferred that the role of hydrophilicity prevails over that of the corrosion resistance in this comparison. It has been previously reported that among the factors affecting the cellular adhesion strength, cell spreading, and proliferation of an implant, the solid surface free energy (hydrophilicity) is the most important aspect, even if the solid surface is covered by a protein layer [36,37]. In summary, this study showed that $ZrTiO_4$ and $ZrTiO_4$–PMMA sol–gel coating is an efficient surface modification approach to improve the biocompatibility of stainless steels.

This is the accepted manuscript (postprint) of the following article:
E. Salahinejad, M.J. Hadianfard, D.D. Macdonald, S. Sharifia(asl), M. Mozafari, K.J. Walker, A. Tahmasbi Rad, S.V. Madihally, D. Vashaee, L. Tayebi, *Surface Modification of Stainless Steel Orthopedic Implants by Sol–Gel $ZrTiO_4$ and $ZrTiO_4$–PMMA Coatings*, Journal of Biomedical Nanotechnology, 9 (2013) 1327-1335.
http://dx.doi.org/10.1166/jbn.2013.1619

4. Conclusions

The roughness, wettability, and corrosion resistance of a stainless steel substrate coated with sol–gel derived inorganic $ZrTiO_4$ and hybrid $ZrTiO_4$–PMMA thin films were studied and correlated with biocompatibility. It was realized that the coatings improve the hydrophilicity and corrosion resistance of the substrate, where the former increases in the order: substrate < $ZrTiO_4$–PMMA < $ZrTiO_4$ and the latter is improved in the order: substrate < $ZrTiO_4$ < $ZrTiO_4$–PMMA. The study of cell viability via quantitative and microscopic approaches indicated that the cytocompatibility is improved in an order similar to that found for the wettability, suggesting the domination of this surface feature. In conclusion, the developed $ZrTiO_4$ and $ZrTiO_4$–PMMA sol–gel coating modified the surface characteristics and improved the biocompatibility of the metallic substrate.

Acknowledgements

This work was partially supported by AFOSR under Grant no. FA9550-10-1-0010, the National Science Foundation (NSF) under Grant no. 0933763, and the Oklahoma Center for Advancement of Science and Technology under Grant no. HR12-023.

References

[1] T. H. Hin, Engineering materials for biomedical applications, World Scientific Publishing Co. Pte. Ltd. **(2004)**.

[2] M. Niinomi, M. Nakai, J. Hieda, Development of new metallic alloys for biomedical applications, Acta Biomater. 8, 3888-3903 **(2012)**.

This is the accepted manuscript (postprint) of the following article:
E. Salahinejad, M.J. Hadianfard, D.D. Macdonald, S. Sharifia(asl), M. Mozafari, K.J. Walker, A. Tahmasbi Rad, S.V. Madihally, D. Vashaee, L. Tayebi, *Surface Modification of Stainless Steel Orthopedic Implants by Sol–Gel $ZrTiO_4$ and $ZrTiO_4$–PMMA Coatings*, Journal of Biomedical Nanotechnology, 9 (2013) 1327-1335.
http://dx.doi.org/10.1166/jbn.2013.1619

[3] J. Zarzycki, Past and present of sol–gel science and technology, J. Sol–gel Sci. Technol. 8, 17-22 **(1997)**.

[4] K.B. Devi, K. Singh, N. Rajendran, Sol–gel synthesis and characterisation of nanoporous zirconium titanate coated on 316L SS for biomedical applications, J. Sol–gel Sci. Technol. 59, 513-520 **(2011)**.

[5] D.V. Shtansky, M.I. Petrzhik, I.A. Bashkova, F.V. Kiryukhantsev-Korneev, A.N. Sheveiko, E.A. Levashov, Adhesion, friction, and deformation characteristics of Ti–(Ca,Zr)–(C,N,O,P) coatings for orthopedic and dental implants, Phys. Solid State 48, 1301-1308 **(2006)**.

[6] E. Salahinejad, M.J. Hadianfard, D.D. Macdonald, I. Karimi, D. Vashaee, L. Tayebi, Aqueous sol–gel synthesis of zirconium titanate ($ZrTiO_4$) nanoparticles using chloride precursors, Ceram. Int. 38, 6145-6149 **(2012)**.

[7] E. Salahinejad, M.J. Hadianfard, D.D. Macdonald, M. Mozafari, D. Vashaee, L. Tayebi, Zirconium titanate thin film prepared by an aqueous particulate sol–gel spin coating process using carboxymethyl cellulose as dispersant, Mater. Lett. 88, 5-8 **(2012)**.

[8] E. Salahinejad, M.J. Hadianfard, D.D. Macdonald, M. Mozafari, D. Vashaee, L. Tayebi, Multilayer zirconium titanate thin films prepared by a sol–gel deposition method, Ceram. Int. 39, 1271-1276 **(2013)**.

[9] G. Kumar, K. N. Prabhu, Review of non-reactive and reactive wetting of liquids on surfaces, Adv. Colloid Interface Sci. 133, 61-89 **(2007)**.

[10] A. Mendez-Vilas, A.B. Jodar-Reyes, M.L. Gonzalez-Martin, Ultrasmall liquid droplets on solid surfaces: production, imaging, and relevance for current wetting research, Small 5, 1366-1390 (2009).

This is the accepted manuscript (postprint) of the following article:
E. Salahinejad, M.J. Hadianfard, D.D. Macdonald, S. Sharifia(asl), M. Mozafari, K.J. Walker, A. Tahmasbi Rad, S.V. Madihally, D. Vashaee, L. Tayebi, *Surface Modification of Stainless Steel Orthopedic Implants by Sol–Gel $ZrTiO_4$ and $ZrTiO_4$–PMMA Coatings*, Journal of Biomedical Nanotechnology, 9 (2013) 1327-1335.
http://dx.doi.org/10.1166/jbn.2013.1619

[11] T. Kokubo, H. Takadama, How useful is SBF in predicting in vivo bone bioactivity?, Biomaterials 27, 2907-2915 **(2006)**.

[12] S. Satapathy, P. Verma, P.K. Gupta, C. Mukherjee, V.G. Sathe, K.B.R. Varma, Structural, dielectric and ferroelectric properties of multilayer lithium tantalate thin films prepared by sol–gel technique, Thin Solid Films 519, 1803-1808 **(2011)**.

[13] F.C. Frank, J.H. Van der Merwe, One-dimensional dislocations. I. static theory, Proc. R Soc. Lond. Series A: Math. Phys. Sci. 198, 205-216 **(1949)**.

[14] J.W. Matthews, Epitaxial Growth. J.W. Matthews (Ed.), Academic Press, New York **(1975)**.

[15] J. Israelachvili, H. Wennerstrom, Role of hydration and water structure in biological and colloidal interactions, Nature 379, 219-225 **(1996)**.

[16] K. Webb, V. Hlady, P.A. Tresco, Relative importance of surface wettabillity and charged functional groups on NIH 3T3 fibroblasts attachment, spreading, and cytosqueletal organisation, J. Biomed. Mater. Res. 241, 422-430 **(1998)**.

[17] N. Sakai, A. Fujishima, T. Watanabe, K. Hashimoto, Enhancement of the photoinduced hydrophilic conversion rate of TiO_2 film electrode surfaces by anodic polarization, J. Phys. Chem. B 105, 3023-3026 **(2001)**.

[18] Y. Tateishi, N. Kai, H. Noguchi, K. Uosaki, T. Nagamura, K. Tanaka, Local conformation of poly(methyl methacrylate) at nitrogen and water interfaces, Polym. Chem. 1, 303-311 **(2010)**.

[19] T.P. Chou, C. Chandrasekaran, S.J. Limmer, S. Seraji, Y. Wu, M.J. Forbess, C. Nguyen, G.Z. Cao, Organic–inorganic hybrid coatings for corrosion protection, J. Non-Cryst. Solids 290, 153-162 **(2001)**.

This is the accepted manuscript (postprint) of the following article:
E. Salahinejad, M.J. Hadianfard, D.D. Macdonald, S. Sharifia(asl), M. Mozafari, K.J. Walker, A. Tahmasbi Rad, S.V. Madihally, D. Vashaee, L. Tayebi, *Surface Modification of Stainless Steel Orthopedic Implants by Sol–Gel $ZrTiO_4$ and $ZrTiO_4$–PMMA Coatings*, Journal of Biomedical Nanotechnology, 9 (2013) 1327-1335.
http://dx.doi.org/10.1166/jbn.2013.1619

[20] D.D. Macdonald, Theoretical investigation of the evolution of the passive state on Alloy 22 in acidified, saturated brine under open circuit conditions, Electrochim. Acta 56, 7411-7420 **(2011)**.

[21] A. Carnot, I. Frateur, S. Zanna, B. Tribollet, I. Dubois-Brugger, P. Marcus, Corrosion mechanisms of steel concrete moulds in contact with a demoulding agent studied by EIS and XPS, Corros. Sci. 45, 2513-2524 **(2003)**.

[22] C. Hitz, A. Lasia, Experimental study and modeling of impedance of the her on porous Ni electrodes, J. Electroanal. Chem. 500, 213-222 **(2001)**.

[23] D.A. López, N.C. Rosero-Navarro, J. Ballarre, A. Durán, M. Aparicio, S. Ceré, Multilayer silica-methacrylate hybrid coatings prepared by sol–gel on stainless steel 316L: Electrochemical evaluation, Surf. Coat. Technol. 202, 2194-2201 **(2008)**.

[24] E. Setare, K. Raeissi, M.A. Golozar, M.H. Fathi, The structure and corrosion barrier performance of nanocrystalline zirconia electrodeposited coating, Corros. Sci. 51, 1802-1808 **(2009)**.

[25] J. Creus, H. Mazille, H. Idrissi, Porosity evaluation of protective coatings onto steel, through electrochemical techniques, Surf. Coat. Technol. 130, 224-232 **(2000)**.

[26] J. Gallardo, A. Duran, J.J. de Damborenea, Electrochemical and in vitro behaviour of sol–gel coated 316L stainless steel, Corr. Sci. 46, 795-806 **(2004)**.

[27] T.P. Chou, C. Chandrasekaran, S. Limmer, C. Nguyen, G.Z. Cao, Organic-inorganic sol-gel coating for corrosion protection of stainless steel, J. Mater. Sci. Lett. 21, 251-255 **(2002)**.

[28] Y. Oshida, A. Hashem, T. Nishihara, M.V. Yapchulay, Fractal dimension analysis of mandibular bones: towards a morphological compatibility of implants, Biomed. Mater. Eng. 4, 397-407 **(1994)**.

This is the accepted manuscript (postprint) of the following article:
E. Salahinejad, M.J. Hadianfard, D.D. Macdonald, S. Sharifia(asl), M. Mozafari, K.J. Walker, A. Tahmasbi Rad, S.V. Madihally, D. Vashaee, L. Tayebi, *Surface Modification of Stainless Steel Orthopedic Implants by Sol–Gel $ZrTiO_4$ and $ZrTiO_4$–PMMA Coatings*, Journal of Biomedical Nanotechnology, 9 (2013) 1327-1335.
http://dx.doi.org/10.1166/jbn.2013.1619

[29] B. Kasemo, J. Gold, Implant surfaces and interface processes, Adv. Dent. Res. 13, 8-20 **(1999)**.

[30] K. Anselme, Osteoblast adhesion on biomaterials, Biomaterials 21, 667-681 **(2000)**.

[31] T.G. Ruardy, J.M. Schakenraad, H.C. Van der Mei, H.J. Busscher, Adhesion and spreading of human skin fibroblasts on physocochemically characterized gradient surfaces, J. Biomed. Mater. Res. 29, 1415-1423 **(1995)**.

[32] A. Georgi, F. Grinnel, T. Groth, Studies on the biocompatibility of materials: fibroblast reorganisation of substratum-bound fibronectin on surfaces varying in wettability, J. Biomed. Mater. Res. 30, 385-391 **(1996)**.

[33] J.Y. Hong, Y.J. Kim, H.W. Lee, Osteoblastic cell response to thin film of poorly crystalline calcium phosphate apatite formed at low temperatures, Biomaterials 24, 2977-2984 **(2003)**.

[34] L. Ponsonnet, K. Reybier, N. Jaffrezic, V. Comte, C. Lagneaub, M. Lissac, C. Martelet, Relationship between surface properties (roughness, wettability) of titanium and titanium alloys and cell behaviour, Mater. Sci. Eng. C 23, 551-560 **(2003)**.

[35] M. Bigerelle, K. Anselme, B. Noël, I. Rudermana, P. Hardouin, A. Iost, Improvement in the morphology of Ti-based surfaces: a new process to increase in vitro human osteoblast response, Biomaterials 23, 1563-1577 **(2002)**.

[36] N. Hallab, K. Bundy, K. O'Connor, R.L. Moses, J.J. Jacobs, Evaluation of metallic and polymeric biomaterial surface energy and surface roughness characteristics for directed cell adhesion, Tissue Eng. 71, 55-71 **(2001)**.

[37] J.M. Schakenraad, H.J. Busscher, Ch.R.H. Wildevuur, J. Arends, Thermodynamic aspects of cell spreading on solid substrata, Cell Biophys. 13, 75-91 **(1988)**.

This is the accepted manuscript (postprint) of the following article:
E. Salahinejad, M.J. Hadianfard, D.D. Macdonald, S. Sharifia(asl), M. Mozafari, K.J. Walker, A. Tahmasbi Rad, S.V. Madihally, D. Vashaee, L. Tayebi, *Surface Modification of Stainless Steel Orthopedic Implants by Sol–Gel $ZrTiO_4$ and $ZrTiO_4$–PMMA Coatings*, Journal of Biomedical Nanotechnology, 9 (2013) 1327-1335.
http://dx.doi.org/10.1166/jbn.2013.1619

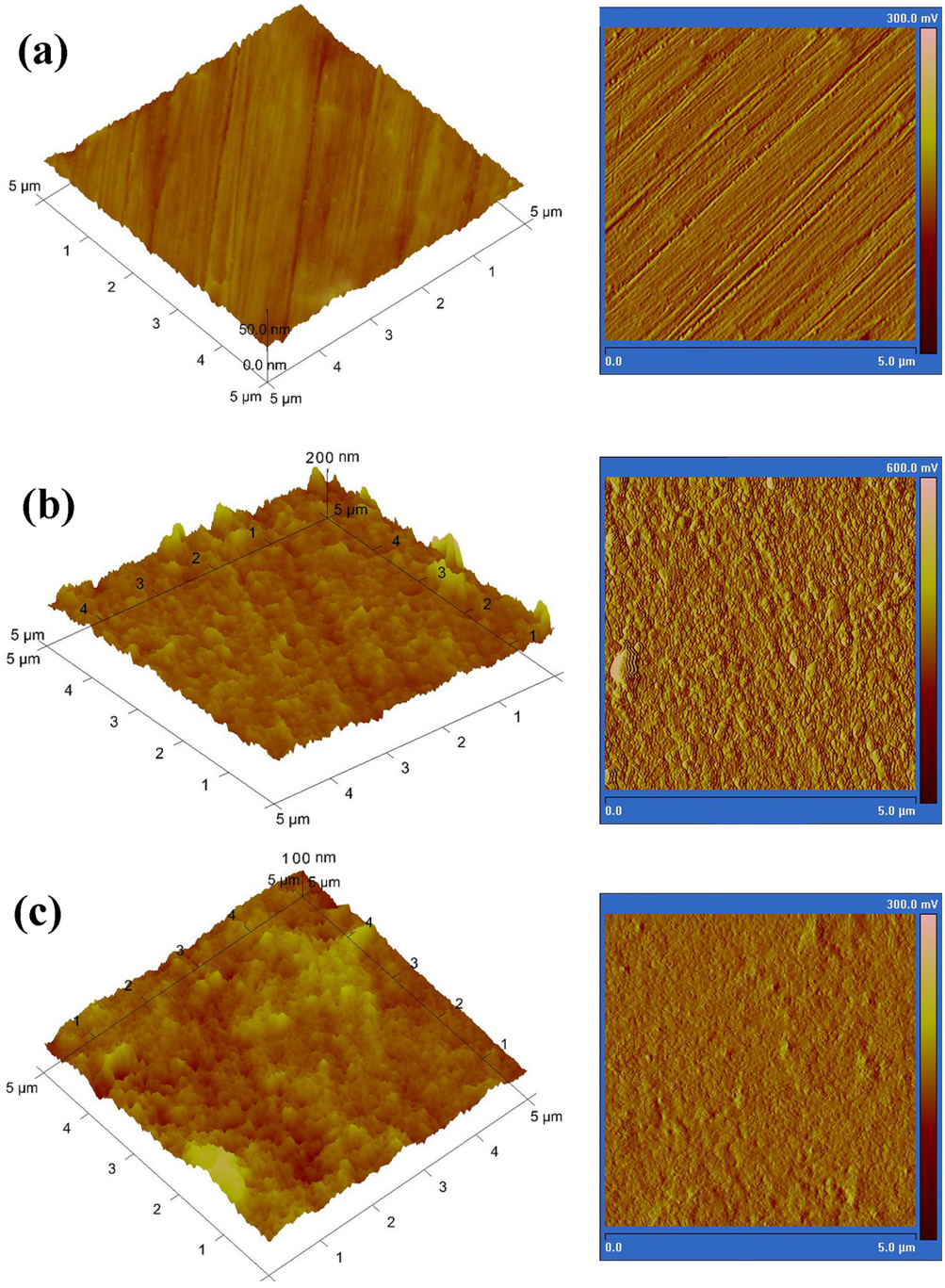

Fig. 1. Two- and three-dimensional AFM images of the stainless steel uncoated (a) and coated with the $ZrTiO_4$ (b) and $ZrTiO_4$–PMMA (c) thin films.

This is the accepted manuscript (postprint) of the following article:
E. Salahinejad, M.J. Hadianfard, D.D. Macdonald, S. Sharifia(asl), M. Mozafari, K.J. Walker, A. Tahmasbi Rad, S.V. Madihally, D. Vashaee, L. Tayebi, *Surface Modification of Stainless Steel Orthopedic Implants by Sol–Gel $ZrTiO_4$ and $ZrTiO_4$–PMMA Coatings*, Journal of Biomedical Nanotechnology, 9 (2013) 1327-1335.
http://dx.doi.org/10.1166/jbn.2013.1619

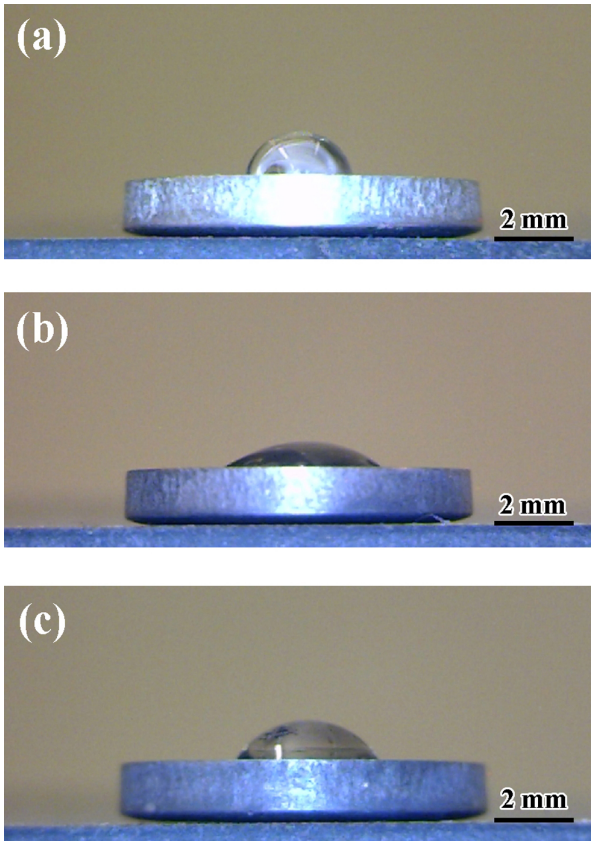

Fig. 2. Water droplets on the stainless steel uncoated (a) and coated with the $ZrTiO_4$ (b) and $ZrTiO_4$–PMMA (c) thin films.

This is the accepted manuscript (postprint) of the following article:
E. Salahinejad, M.J. Hadianfard, D.D. Macdonald, S. Sharifia(asl), M. Mozafari, K.J. Walker, A. Tahmasbi Rad, S.V. Madihally, D. Vashaee, L. Tayebi, *Surface Modification of Stainless Steel Orthopedic Implants by Sol–Gel $ZrTiO_4$ and $ZrTiO_4$–PMMA Coatings*, Journal of Biomedical Nanotechnology, 9 (2013) 1327-1335.
http://dx.doi.org/10.1166/jbn.2013.1619

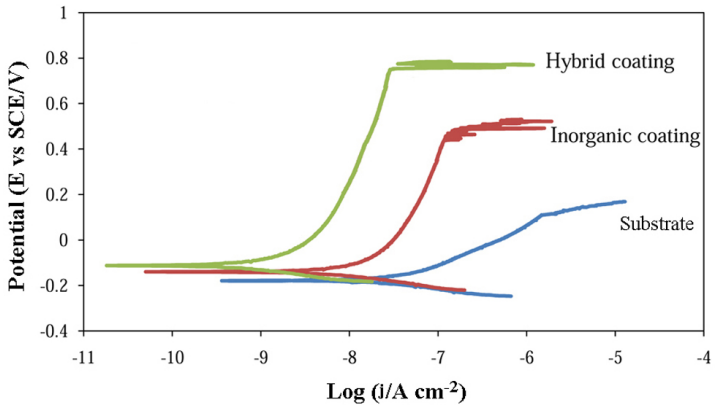

Fig. 3. Anodic potentiodynamic polarization curves of the samples in SBF.

This is the accepted manuscript (postprint) of the following article:
E. Salahinejad, M.J. Hadianfard, D.D. Macdonald, S. Sharifia(asl), M. Mozafari, K.J. Walker, A. Tahmasbi Rad, S.V. Madihally, D. Vashaee, L. Tayebi, *Surface Modification of Stainless Steel Orthopedic Implants by Sol–Gel $ZrTiO_4$ and $ZrTiO_4$–PMMA Coatings*, Journal of Biomedical Nanotechnology, 9 (2013) 1327-1335.
http://dx.doi.org/10.1166/jbn.2013.1619

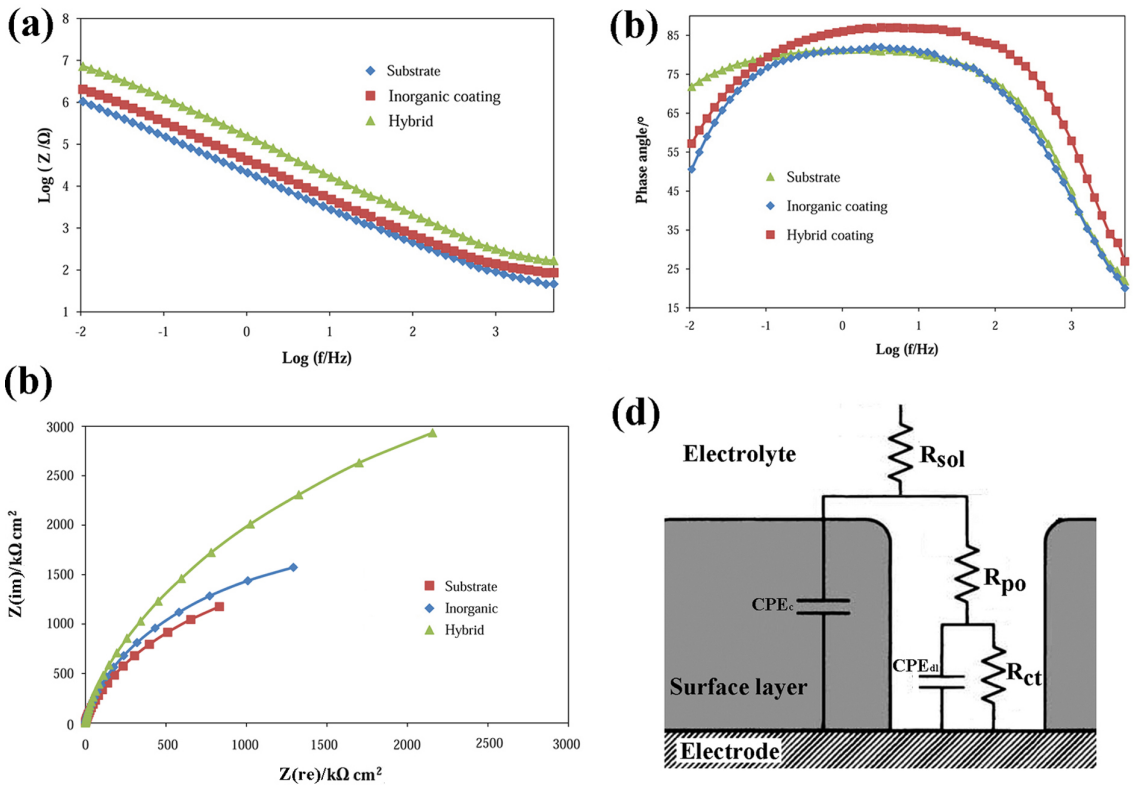

Fig. 4. (a) Bode impedance, (b) Bode phase angle, and (c) Nyquist plots; and (d) equivalent electrical circuit used for the quantitative analyses of the impedance spectra.

This is the accepted manuscript (postprint) of the following article:
E. Salahinejad, M.J. Hadianfard, D.D. Macdonald, S. Sharifia(asl), M. Mozafari, K.J. Walker, A. Tahmasbi Rad, S.V. Madihally, D. Vashaee, L. Tayebi, *Surface Modification of Stainless Steel Orthopedic Implants by Sol–Gel $ZrTiO_4$ and $ZrTiO_4$–PMMA Coatings*, Journal of Biomedical Nanotechnology, 9 (2013) 1327-1335.
http://dx.doi.org/10.1166/jbn.2013.1619

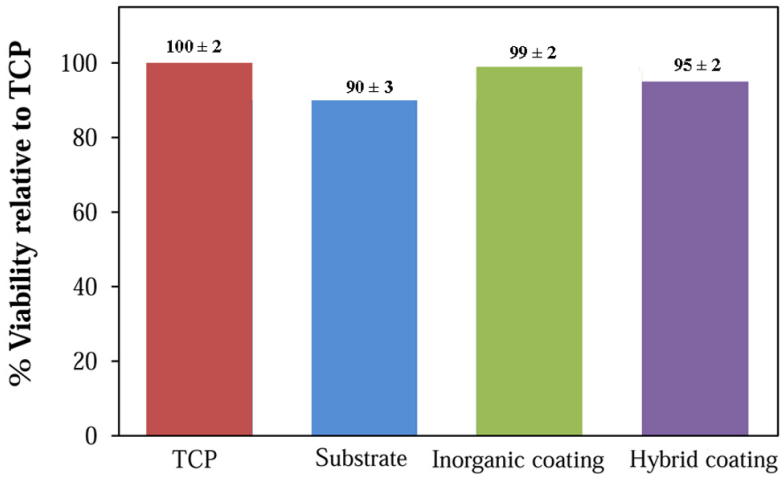

Fig. 5. Cell viability on the specimens after one day, determined by fluorescence in the cytoplasmic extract.

This is the accepted manuscript (postprint) of the following article:
E. Salahinejad, M.J. Hadianfard, D.D. Macdonald, S. Sharifia(asl), M. Mozafari, K.J. Walker, A. Tahmasbi Rad, S.V. Madihally, D. Vashaee, L. Tayebi, *Surface Modification of Stainless Steel Orthopedic Implants by Sol–Gel $ZrTiO_4$ and $ZrTiO_4$–PMMA Coatings*, Journal of Biomedical Nanotechnology, 9 (2013) 1327-1335.
http://dx.doi.org/10.1166/jbn.2013.1619

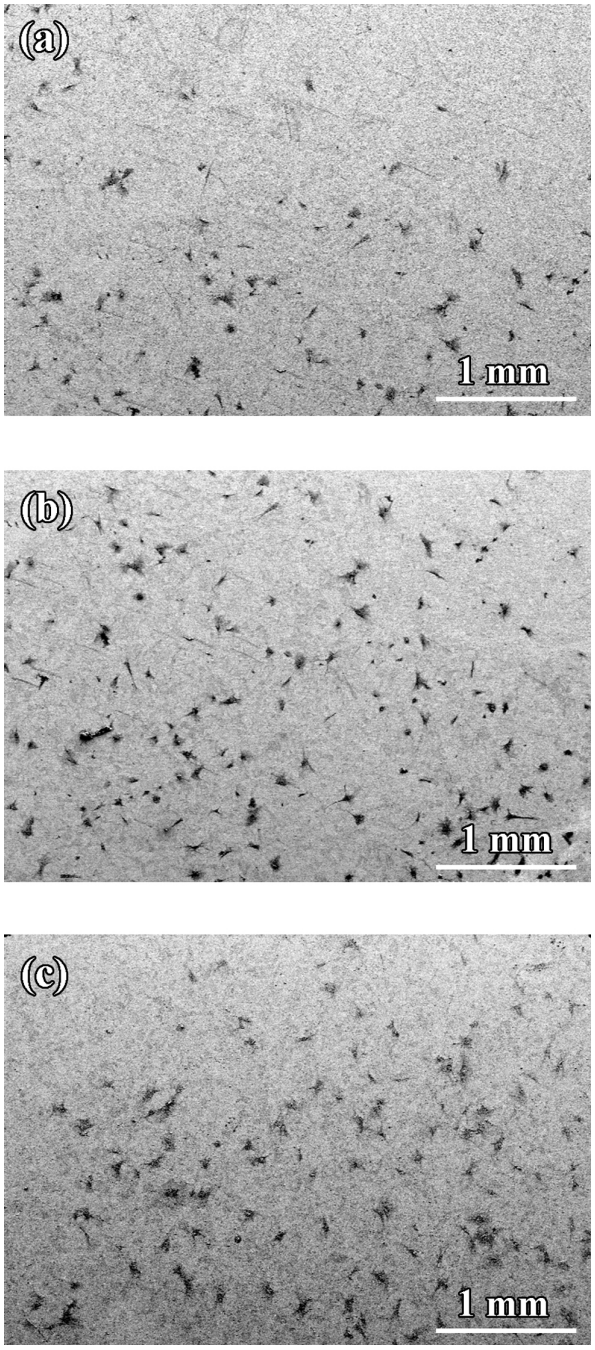

Fig. 6. Low-magnification SEM micrograph of cells fixed on the stainless steel uncoated (a) and coated with the $ZrTiO_4$ (b) and $ZrTiO_4$–PMMA (c) thin films.

This is the accepted manuscript (postprint) of the following article:
E. Salahinejad, M.J. Hadianfard, D.D. Macdonald, S. Sharifia(asl), M. Mozafari, K.J. Walker, A. Tahmasbi Rad, S.V. Madihally, D. Vashaee, L. Tayebi, *Surface Modification of Stainless Steel Orthopedic Implants by Sol–Gel $ZrTiO_4$ and $ZrTiO_4$–PMMA Coatings*, Journal of Biomedical Nanotechnology, 9 (2013) 1327-1335.
http://dx.doi.org/10.1166/jbn.2013.1619

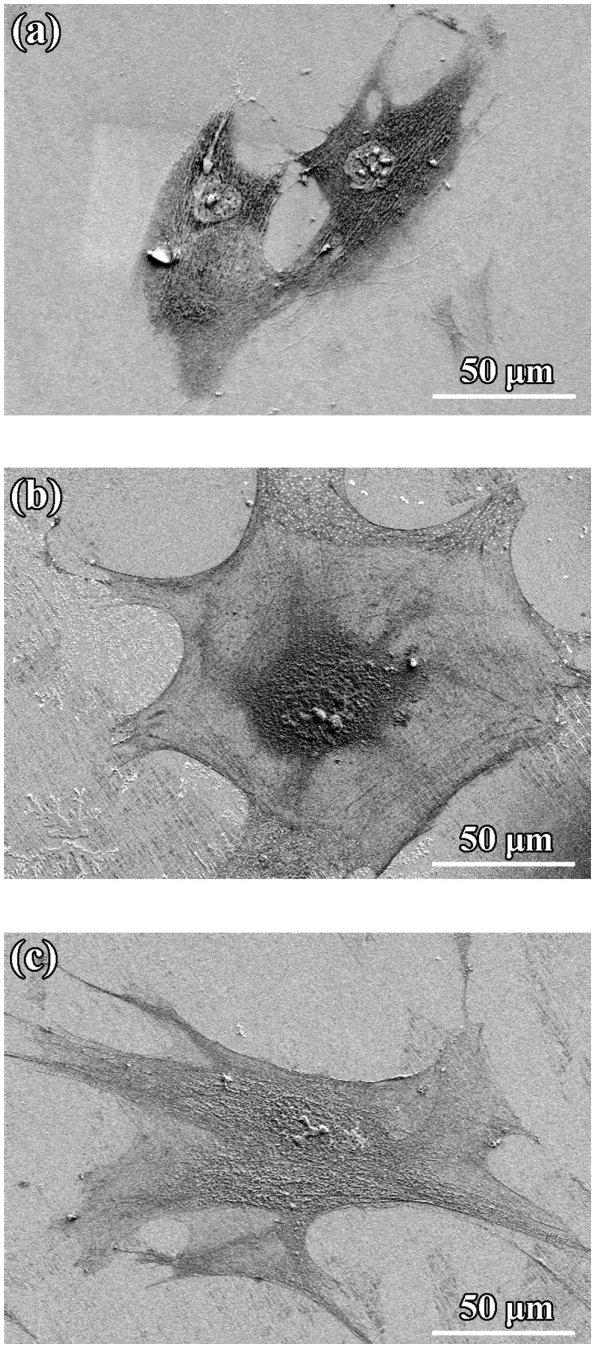

Fig. 7. SEM micrograph of cells fixed on the stainless steel uncoated (a) and coated with the $ZrTiO_4$ (b) and $ZrTiO_4$–PMMA (c) thin films.

This is the accepted manuscript (postprint) of the following article:
E. Salahinejad, M.J. Hadianfard, D.D. Macdonald, S. Sharifia(asl), M. Mozafari, K.J. Walker, A. Tahmasbi Rad, S.V. Madihally, D. Vashaee, L. Tayebi, *Surface Modification of Stainless Steel Orthopedic Implants by Sol–Gel $ZrTiO_4$ and $ZrTiO_4$–PMMA Coatings*, Journal of Biomedical Nanotechnology, 9 (2013) 1327-1335.
http://dx.doi.org/10.1166/jbn.2013.1619

Tables

Table 1. Nominal ion concentration/mmol dm^{-3} of SBF and human blood plasma [11].

Ion	*Plasma*	*SBF*
Na^+	142.0	142.0
K^+	5.0	5.0
Mg^{2+}	1.5	1.5
Ca^{2+}	2.5	2.5
Cl^-	103.0	147.8
HCO_3^-	27	4.2
HPO_4^{2-}	1.0	1.0
SO_4^{2-}	0.5	0.5

Table 2. Equivalent electrical circuit parameters obtained by the impedance studies.

Sample	R_{po} (Ω cm^2)	Q_c ($\mu\Omega^{-1}$ $s^{n1}cm^{-2}$)	n_c	R_{ct} ($M\Omega$ cm^2)	Q_{dl} ($\mu\Omega^{-1}$ $s^{n1}cm^{-2}$)	n_{dl}	Residual error
Substrate	60.0 ± 12.2	2.8 ± 0.3	0.88 ± 0.03	1.5 ± 0.3	10.4 ± 1.1	0.99 ± 0.05	$7.8 * 10^{-5}$
Inorganic	119.8 ± 10.5	2.9 ± 0.2	0.92 ± 0.03	2.3 ± 0.1	5. 3 ± 0.4	0.90 ± 0.05	$6.8 * 10^{-5}$
Hybrid	211.2 ± 17.0	1.6 ± 0.5	0.98 ± 0.02	3.5 ± 0.2	2.0 ± 0.5	0.87 ± 0.03	$9.5 * 10^{-5}$